NUKLEONIKA 2006;51(3):169–173

ORIGINAL PAPER

Monte-Carlo simulations of a neutron source generated with electron linear accelerator

Adam Wasilewski,
Sławomir Wronka

Abstract Neutron generator consisting of an electron linear accelerator and a tungsten X-ray converter can produce a neutron flux of 10^9 n/s and 10^{11} n/s at electron energies of 10 and 15 MeV, respectively, with an electron beam intensity of 10^{14} e/s which means 160 and 240 W of electron incident beam power, respectively. Two stage neutron production with an electron to photon natural tungsten converter and a photon to neutron ^{9}Be converter are equal or less efficient than one stage tungsten converter only. There is a low neutron separation energy of ^{9}Be and a small cross section for the photonuclear reaction $\gamma(^9\mathrm{Be},^8\mathrm{Be}^*)$n in comparison to photonuclear cross section in all tungsten isotopes for the photon energy range in and below resonance region. Results of the neutron generator modeling performed with the Fluka Monte-Carlo code are presented in this article.

Key words Fluka • Monte-Carlo simulations • neutron generation • electron linear accelerator • X-ray converter

A. Wasilewski✉, S. Wronka
Establishment for Nuclear Equipment,
The Andrzej Sołtan Institute for Nuclear Studies,
05-400 Otwock-Świerk, Poland,
Tel.: +48 22 718 05 22, Fax: +48 22 718 05 01,
E-mail: adamw@ipj.gov.pl

Received: 7 November 2005
Accepted: 30 May 2006

Introduction

Electron linear accelerators are widely used in medicine and in industry. Typically, the obtained electron energies are below 20 MeV and the accelerator power reaches a few hundred kW. An electron beam can be used to produce bremsstrahlung photons which, in turn, can evoke neutron emission in materials with low neutron separation energy. Consequently, a photoneutron beam can be generated in photonuclear reaction [7, 10, 11]. The energy spectrum of bremsstrahlung photons is continuous with a domination of low energies [2, 8, 9].

In the neutron production typical materials, used as the conversion targets, are beryllium and deuterium. Neutron separation energy of ^{9}Be is equal to 1.67 MeV, while for ^{2}H it is equal to 2.23 MeV. Unfortunately, the conversion efficiency of electrons to photons in the bremsstrahlung process for both deuterium and beryllium (low-Z) is very small. Hence, a double converter can be constructed using a combination of high-Z material, like tungsten, to obtain high flux of bremsstrahlung photons and low neutron separation energy material to maximize a number of neutrons.

Production of neutrons with an electron linac with low-Z conversion targets has been discussed in [1, 4, 12]. In this work, neutron production with high-Z materials and electrons with energy range up to 15 MeV was studied. The photonuclear cross section is at least

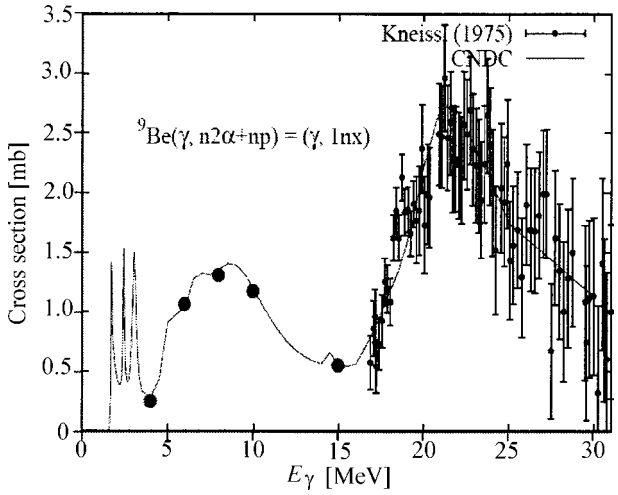

Fig. 1. Comparison of simulation by Fluka and theoretical calculation of cross section for the reaction $\gamma(^9Be,^8Be^*)n$. Points with a photon energy of 4, 6, 8, 10 and 15 MeV are the results obtained from Fluka. The figure is taken from page 96 in Ref. [3]. Reproduced by permission of the International Atomic Energy Agency.

two orders of magnitude higher for high-Z materials than for materials with low-Z [3].

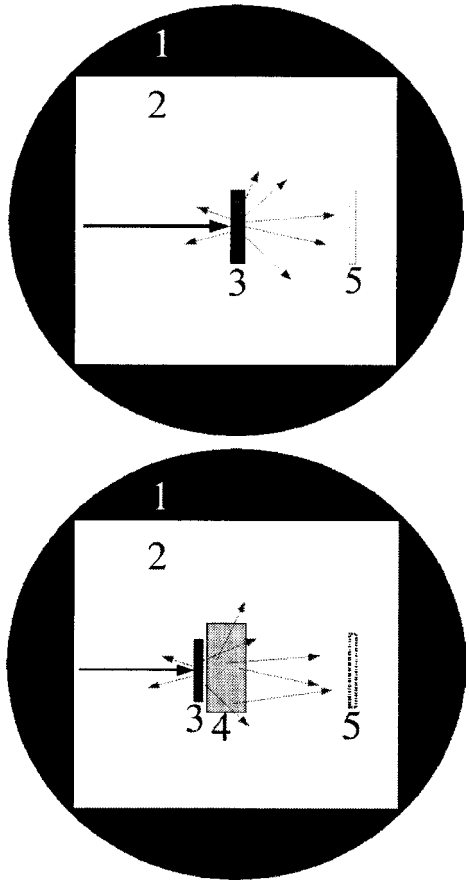

Fig. 2. Geometry of the system used in simulation with the Fluka Monte-Carlo code. The thick arrow indicates electron beam, the thin arrows indicate reaction products. Region definition: 1 – Black hole – infinite sphere; 2 – vacuum – infinite cube inside Black hole; 3 – tungsten or lead converter – 10 cm radius roller; 4 – beryllium converter – 10 cm radius cylinder; 5 – detection region 40 × 40 cm. Pictures are not in scale.

Monte-Carlo simulations

Production of photoneutrons has been theoretically modeled using the Monte-Carlo code Fluka [5]. First, the Fluka code was verified by various simulation of reaction known in the literature, an example is shown in Fig. 1. Then, Fluka was used for neutron generation simulations.

Single, high-Z converter (tungsten, lead) and a double converter: a combination of high-Z (tungsten) and low-Z (beryllium) materials were considered. In both cases the number of electrons, photons and neutrons as well as the energy spectra of secondary particles were simulated. All simulations were performed for 10 MeV and 15 MeV electron beams, monoenergetic and with Gaussian energy distribution of 1 MeV FWHM.

System geometry is shown in Fig. 2. On the top, the geometry with a single converter is presented, and below, the geometry with separated electron to photon and photon to neutron converters is shown.

Detection of all particles takes place in the 40 × 40 cm detection plane, placed 1 m from the nearest boundary of the nearest converter at the border of regions 5 and 2. The input files for Fluka code used for calculations allow to obtain flux and energy spectrum of produced particles.

Results and discussion

Single converter

Electrons, photons and neutrons are detected after a single tungsten or lead converter being bombarded by 10^{14} electrons of energy 10 MeV or 15 MeV. The numbers of photons and electrons behind the target are presented in Figs. 3 and 4, respectively, as a function of target thickness.

The total neutron production is presented in Fig. 5. The neutron flux produced by 15 MeV electron beam is around 20 times larger than produced by 10 MeV electron beam. There is no major difference between

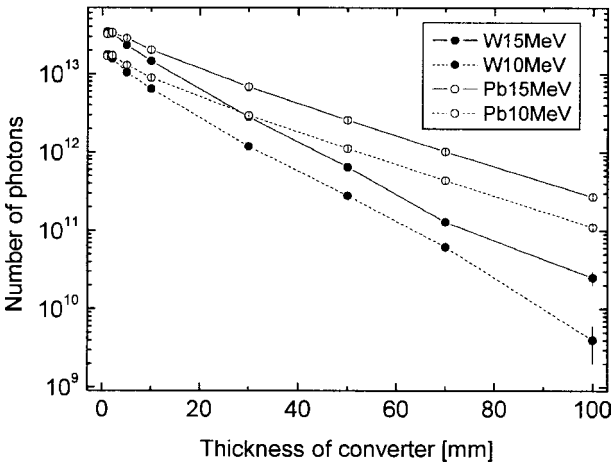

Fig. 3. Photon production inside the lead and tungsten converters bombarded by 10^{14} monoenergetic 10 MeV and 15 MeV electrons. Detection in the detection plane. Maximum emission is observed for 1 mm of tungsten and 2 mm of lead.

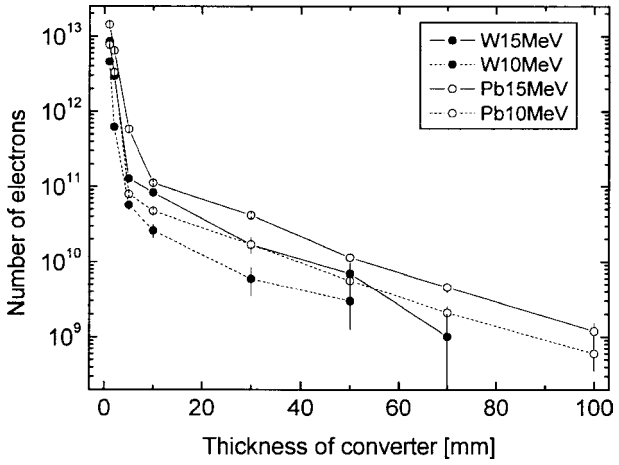

Fig. 4. Number of survival-and-secondary electrons behind the tungsten and lead converters bombarded by 10^{14} monoenergetic 10 MeV and 15 MeV electrons. The number of electrons registered in the detection plane systematically decreases with increasing the conversion target thickness.

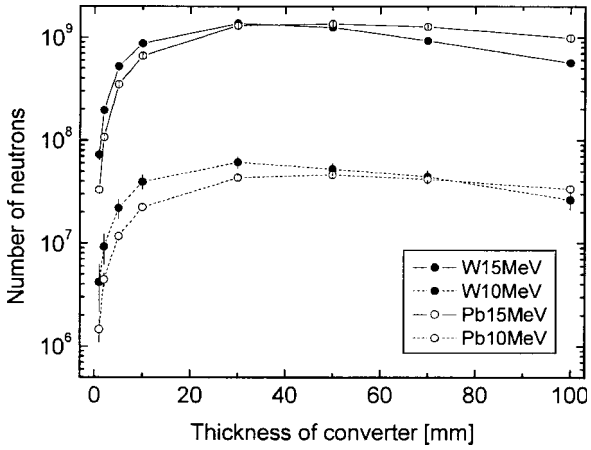

Fig. 5. Number of neutron detected behind the tungsten and lead converters bombarded by 10^{14} monoenergetic 10 MeV and 15 MeV electrons. Detection in the detection plane.

the electron to neutron conversion efficiency for lead and tungsten. Optimal converter thickness for maximum neutron yield is about 3 cm for tungsten and 5 cm for lead. These numbers are similar for 10 MeV and for 15 MeV.

The yield of all particles increases with electron energy. The neutron flux generated in the lead converter is smaller than that generated in tungsten for lower thicknesses (see Fig. 5), while the photon flux is much higher in the whole range of thicknesses (see Fig. 3).

In Fig. 6, the energy spectra of photons and neutrons generated on tungsten converter for both 10 MeV and 15 MeV electron beams are presented for two converter thicknesses. The flux of photons decreases as a function of thickness of the converter, while for neutrons the flux increases with thickness.

As one can see in Fig. 6, the shape of spectrum for 3 cm thickness of tungsten is slightly different than for 1 mm. Medium and most probable energy of neutrons is shifted to lower energy for 3 cm of tungsten in comparison to 1 mm of tungsten.

Photonuclear reaction with neutron production is only possible when the energy of initial photon is greater

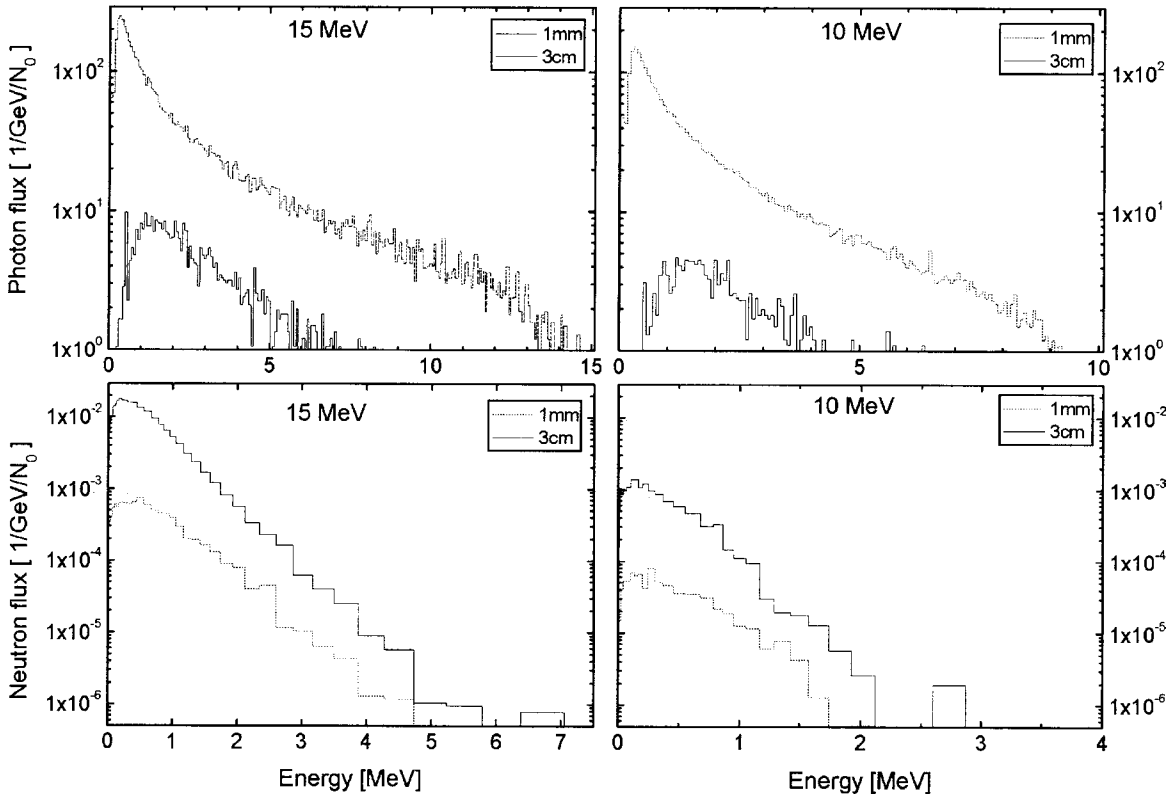

Fig. 6. Energy spectra of produced photons (the first raw) and neutrons (the second raw) for 10 MeV electron beam (right column) and 15 MeV electron beam (left column) for two arbitrary chosen tungsten converter thickness (1 mm and optimal for neutron yield 3 cm).

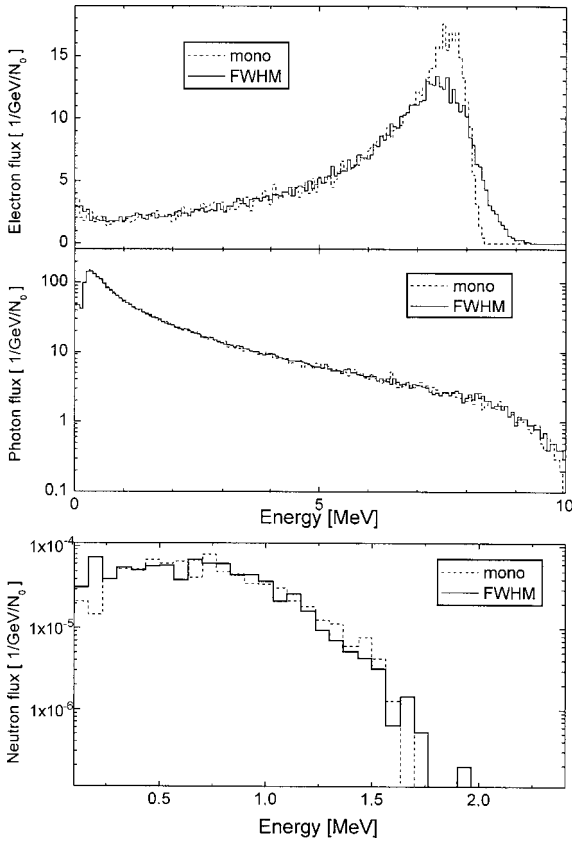

Fig. 7. Energy spectra of electrons, photons and neutrons observed behind a 1 mm tungsten conversion target bombarded by 10 MeV electron beam. The Gaussian energy distribution beam with FWHM 1 MeV is represented by the solid line (marked as FWHM), while the monoenergetic beam by the doted line (marked as mono).

than neutron separation energy. Neutron separation energies for tungsten and lead isotopes are in the range of 6–9 MeV (8.4 MeV – ^{180}W, 8.1 MeV – ^{182}W, 6.2 MeV – ^{183}W, 7.4 MeV – ^{184}W, 7.2 MeV – ^{186}W and 8.4 MeV – ^{204}Pb, 8.1 MeV – ^{206}Pb, 6.7 MeV – ^{207}Pb, 7.4 MeV – ^{208}Pb) [6]. The neutron separation energy can explain the maximum energy of generated neutrons. If the beam energy is 10 MeV, then the maximal possible energy of neutrons generated in tungsten is 3.8 MeV, as one can see from the difference between beam energy and neutron separation energy for ^{183}W. If the beam energy is 15 MeV, then the energy of generated neutrons cannot be greater than 8.8 MeV.

Energy spectra of secondary particles generated by the primary electron 10 MeV beam, for both monoenergetic and Gaussian energy distribution with FWHM 1 MeV beams, on the 1 mm tungsten conversion target are shown in Fig. 7. As one can see, there is no significant difference in the results while the primary beam energy distribution changes from monoenergetic to Gaussian.

Double converter

Neutron production in beryllium induced by photons produced in a thin high-Z target was generated as a function of Be thickness and as a function of first target thickness, see Fig. 2. Results are presented in Fig. 8.

As one can see in Fig. 8, the beryllium layer does not increase the neutron flux. For low Be thicknesses (up to 50 mm), the neutron flux remains nearly constant and is equal to the neutron flux generated only with the tungsten converter. For higher Be thicknesses, the

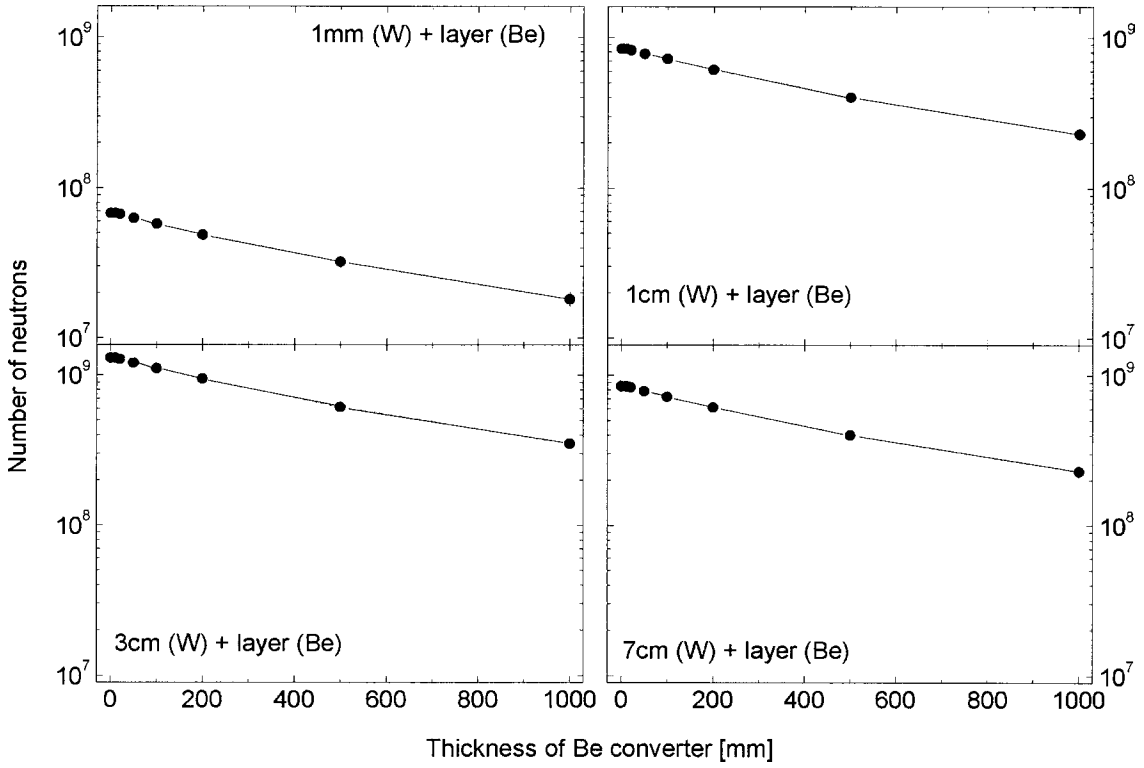

Fig. 8. Neutron production by 10^{14} electron beam with energy 15 MeV in the beryllium converter after 1 mm, 1 cm, 3 cm and 7 cm of tungsten converter. Detection in the detection plane.

neutron flux observed in the detection plane decreases with thickness due to neutron scattering on beryllium nuclei.

Conclusions

The obtained results of performed Monte-Carlo simulations indicate that the largest number of neutrons can be generated in a single, high-Z converter (tungsten, lead), when the conversion target thickness is in the 3 to 5 cm range. Using electron beam with energy of 15 MeV and intensity $\sim 10^{14}$ e/s, the flux of $\sim 10^9$ n/s is generated in the 40×40 cm detection field at a distance of 1 m from the conversion target. Using the 10 MeV electron beam, the flux $\sim 5 \times 10^7$ n/s is generated within the same field.

Photon spectra generated by Monte-Carlo simulations have typical energy distribution characteristics for the bremsstrahlung process. Calculated neutron and photon fluxes and obtained energy spectra do not depend on the diffusion of primary electron beam energy.

No considerable increase of the neutron flux has been observed when two conversion targets have been used, the first made of tungsten to generate photons, and the second made of beryllium to generate photoneutrons. The increase of the beryllium converter thickness causes an increase of neutron scattering and results in a decrease of the neutron flux in the detection field. The increase of thickness of the first converter does not change the characteristic decrease of neutron flux with increasing the second beryllium converter.

References

1. Akkurt I, Adler J-O, Annand JRM *et al*. (2003) Photoneutron yields from tungsten in the energy range of the giant dipole resonance. Phys Med Biol 48:3345–3352
2. Berger JM (1957) Computation of nonrelativistic electron bremsstrahlung. Phys Rev 105:35–38
3. Chadwick MB, Oblozinsky P, Blokhin AI *et al*. (2000) Handbook on photonuclear data for applications cross-sections and spectra. IAEA-TECDOC-1178. IAEA, Vienna
4. Dale GE, Gahl JM (2002) Preliminary modeling results of a thermal neutron source driven with electron linac. In: Mehlhorn TA, Sweeney MA (eds) Proc of the 14th Int Conf on High-Power Particle Beams. American Institute of Physics, pp 369–372
5. Fasso A, Ferrari A, Ranft J, Sala P (2005) Code Fluka 2003 version 1.0b, Mar-04, http://www.fluka.org/
6. Firestone RB, Shirley VS (eds) (1996) Table of isotopes, 8th ed. John Wiley & Sons Inc, New York
7. Gibbons JH, Macklin RL, Marion JB, Schmitt HW (1959) Precision measurement of the $Be^9(\gamma,n)$ cross section. Phys Rev 114:1319–1323
8. Haug E (2003) Photon energy spectrum of electron-positron bremsstrahlung in the center-of-mass system. Eur Phys J C 31:365–369
9. Haug E (2003) Proton-electron bremsstrahlung. Astron Astrophys 406:31–35
10. John W, Prosser JM (1962) Photodisintegration cross section of beryllium near threshold. Phys Rev 127:231–235
11. Kneissl U, Kuhl G, Leister KH, Weller A (1975) Photoneutron cross section for ^{9}Be obtained with quasimonoenergetic photons. Nucl Phys A 247:91–102
12. Konefał A, Dybek M, Zipper W, Łobodziec W, Szczucka K (2005) Thermal and epithermal neutrons in the vicinity of the Primus Siemens biomedical accelerator. Nukleonika 50:73–81